Dedicated to Academician Aureliu Sandulescu's 80^{th} Anniversary

SYSTEMATICS OF HINDRANCE FACTORS IN ALPHA DECAY OF EVEN-EVEN TRANS-LEAD NUCLEI

D. BUCURESCU[a], N.V. ZAMFIR[b]

Horia Hulubei National Institute for Physics and Nuclear Engineering,
P.O.B. MG-6, 077125 Măgurele, Bucharest, Romania
Email: [a]bucurescu@tandem.nipne.ro; [b]zamfir@tandem.nipne.ro

Received November 3, 2011

The experimental values of the hindrance factors in the alpha decay of even-even trans-lead nuclei, corresponding to the states 2_1^+, 4_1^+, 6_1^+, 0_2^+, and 1_1^- are examined as a function of the mass number and collectivity indicators N_pN_n and P. Their evolution is discussed in connection with the main trends of the collectivity in this region.

Key words: Even-even actinides, alpha decay hindrance factors, experimental systematics.

PACS: 23.60.+e, 21.10.Re, 27.90.+b.

1. INTRODUCTION

Alpha decay is one of the oldest observed nuclear structure phenomena, but it is still important as an experimental tool for investigating unstable nuclei, especially in the heavy and superheavy regions. The calculation of the absolute values of the alpha decay rates is a problem that is still not fully solved. Experimentalists often need tools to evaluate expected alpha decay rates for nuclei that are not studied yet. Empirical systematics, such as the Geiger-Nuttall law [1], or its generalization by Viola and Seaborg [2] are very useful in this respect. Another aspect is that the most studied alpha decay processes are those implying the unhindered transitions (with $L = 0$), that are mostly measured for the ground state to ground state transition of even-even nuclei. By contrast, the population of excited states in the daughter nuclei (the fine structure of α-decay), especially for non-zero spin states is much less studied both experimentally and theoretically.

In the present work we review the up-to-date experimental data on the α-decay fine structure for the even-even nuclei above lead. We propose a systematic of the hindrance factors known for excited states based on the N_pN_n scheme [3], and highlight a striking behavior of the hindrance factors for the lowest members of the ground state band of the rotational nuclei from this region.

2. THE ANALYZED EXPERIMENTAL DATA

The considered alpha-decay data were those of the even-even parent nuclei with $Z \geq 84$ for which at least the branch for the 2_1^+ state was measured besides that of the

ground state. In addition to the 2_1^+ state, other states considered in our analysis were the 4_1^+ and 6_1^+ states that were measured in most of the rotational nuclei, and also the 0_2^+ and 1_1^- states (less numerous data). For all these states we have examined the measured hindrance factors. Systematics of these quantities were published before by Ellis and Schmorak [4] (for $A \geq 229$), and by Akovali [5], but we have also checked these experimental data with the most recent ENSDF evaluations [6].

The hindrance factors HF in the alpha decay have the following definition:

$$HF = T_{1/2}(\alpha)_{exp.}/T_{1/2}(\alpha)_{theor.}$$

where $T_{1/2}(\alpha)_{exp.}$ is the partial half-life for the excited state having a given α - decay branch ($T_{1/2}(\alpha)_{exp.} = T_{1/2}/\alpha - branch$). Because they comprise a theoretically calculated quantity, they are model dependent. In the convention adopted by the ENSDF (therefore, for all HF's considered by us) the theoretical half-life $T_{1/2}(\alpha)_{theor.}$ is obtained from the spin-independent equations of Preston [7]. Moreover, for the even-even nuclei, the HF for the ground state to ground state ($0^+ \rightarrow 0^+$) transition is taken 1 by definition, therefore all other hindrance factors are relative to this value. By this procedure, the hindrance factors are basically an $\alpha-$decay half-life corrected for the barrier penetration, leaving only the dependence on the structure of the initial and final states. This makes the α-decay a strong spectroscopic tool for investigating the properties of the nuclear states.

In total, we have found experimental HF values for 62 2_1^+ states, 29 4_1^+ states, 17 6_1^+ states, 11 0_2^+ states, and 15 1_1^- states, respectively, in daughter nuclei with $Z \geq 82$. Hindrance factors are also known for other excited states in this set of considered nuclei, but in smaller numbers.

3. SYSTEMATICS OF THE HINDRANCE FACTORS

In this section we examine the evolution of the experimental hindrance factors from the set defined above, as a function of different structure parameters. Fig. 1 shows the HF values for the first excited state (the 2_1^+ state). The upper panel displays the evolution with the mass number A of the daughter nucleus. It shows a rather smooth evolution, at least above $A = 220$, but this representation has the disadvantage that it does not distinguish between isobars.

We have represented the same HF values against two other quantities, known to describe very well the development and evolution of collectivity over wide nuclear regions. The first of these is the product N_pN_n, between the numbers of active protons (N_p) and neutrons (N_n), as counted with respect to the nearest magic number. This product, roughly proportional to the strength of the neutron-proton interaction, was shown to give very compact trajectories for the evolution of many structure indicators, such as the ratio $R(4/2) = E(4_1^+)/E(2_1^+)$, the electromagnetic transition

probability $B(E2; 2_1^+ \to 0_1^+)$, *etc*. [3, 8]. It can be seen (the middle panel of Fig. 1) that the representation after N_pN_n is useful, because at least for the collective nuclei (N_pN_n larger than about 80) all values follow a rather compact trajectory (in this case, an exponential increase). A similar representation is shown in the bottom panel, against the quantity $P = N_pN_n/(N_p + N_n)$, which roughly represents the ratio between the strengths of the neutron-proton and pairing interactions, and is also a very useful parameter, giving rather compact trajectories for the evolution of various structure indicators over different mass regions [9]. One sees that the P-representation of the HF-values also leads to a nice exponential trajectory for P-values above 3–4 that characterize the collective nuclei [9]. One should emphasize that in Fig. 1 the number of active nucleons (particles or holes) were counted for the daughter nuclei, with respect to the shell gap numbers 82 and 114 for protons, and 126 and 184 for neutrons, respectively.

In Fig. 2 we compare the two representations (N_pN_n and P) for the hindrance factor of the 2_1^+ state, in both situations, when we count the number of active particles either in the daughter nuclei, or in the parent ones. It appears that counting the number of active particles in the daughter nuclei provides slightly smoother trajectories, therefore in the following we will adopt this choice.

Fig. 3 shows the systematic of the $HF(4_1^+)$ values. Again, the N_pN_n or the P-representations lead to relatively smooth trajectories, emphasizing that this way of representing the data may be valuable for predicting expected values for other nuclei. It is worth to mention that the behavior for the 4_1^+ state is completely different from the one of the 2_1^+ state (Fig. 1).

In the following, we adopt these two schemes (representations) also for other states.

4. DISCUSSION

Figure 4 shows a comparison of the evolution of the known HF-values for the 2_1^+, 4_1^+ and 6_1^+ states from the ground state band, in the N_pN_n-scheme. Fig. 5 shows the same data, but represented in the P-scheme. In both cases, the three states show very different behaviors. As remarked above, the 2^+ state shows a practically exponential increase for the deformed nuclei (large N_pN_n, or P values). Over the same interval of N_pN_n or P-values, the 4^+ state shows a marked maximum (around $N_pN_n \approx 250$, corresponding to $P \approx 7.5$). Between $P \approx 4$ and the maximum at $P \approx 7.5$, $HF(4_1^+)$ increases by almost two order of magnitudes, very different from the increase by a factor of about 3 of the 2^+ state. The 6^+ state shows yet a different behavior, in the P interval from about 4 to 7 being out of phase with the 4^+ state: it decreases by more than one order of magnitude, with a possible increase for $P > 7$. These different behaviors of the three states are also clear in the representations as a

function of the mass number shown in the systematic survey of Ref. [4].

Fig. 6 shows the P-systematics of the HF for the second excited 0^+ state (0_2^+) and the 1_1^- state. The number of such states with measured HF is smaller in this case therefore it seems premature to speculate about the occurrence of certain structures.

The very different behaviors of the HF values of the 2^+, 4^+, 6^+ states from the ground state band is so conspicuous that it calls for a simple explanation, or some correlation with the evolution of other structure indicators of these nuclei. Efforts in this direction were recently made in Refs. [10, 11], where alpha-decay widths for the 2^+ and 4^+ states of nuclei in this mass region were calculated within the stationary coupled channels approach, describing the collective states with the rigid rotor model. A good description for the decay widths of the 2^+ state was obtained [10], while for the 4^+ state a good agreement was obtained only for the $Z = 90$ isotopes but the calculations fail by about 1.5 orders of magnitude in the region of the peak observed around $Z = 94$ (corresponding to the peak in Figs. 4 and 5). In Ref. [11], interesting correlations were observed between the alpha-decay widths and the deformation parameters predicted by the calculations of [12]. The decay widths for the 2^+ states were found rather well correlated with the quadrupole deformation parameter β_2. A certain correlation is also observed between the decay widths of the 4^+ state and the hexadecapole deformation parameter β_4 predicted in [12], but not as good as in the 2^+ state case, and the large discrepancy between experiment and theory in the region of the peak at $Z \approx 94$ still remained.

In the following we discuss the properties of the nuclei from this region by examining some of their low-excitation energy observables. Figure 7 shows such quantities, either experimentally measured or derived from the energies of the ground state band. One of these is the moment of inertia (MoI). Fig. 7(a) shows the experimental MoI as derived from the energy of the 2_1^+ state with the rotor model formula [$J = \hbar^2 I(I+1)/2E(2^+)$], normalized to the MoI calculated for a rigid ellipsoid having a β_2 deformation equal to either the experimental value (as extracted from the tables of [13]) or, when the experimental value was not known, as predicted by [12]. One can see that roughly after the $P = 6$ value the moment of inertia stabilizes at a maximum value which is about half the rigid-body value, similar to the situation from the deformed rare-earth nuclei (fig. 11.2 of [14]). More details about how the rotational properties of these nuclei change with the number of nucleons can be inferred from the graphs (b) and (c) of Fig. 7, which show the two Harris parameters J_0 and J_1 resulted from a fit of the g.s.b. energies with the VMI formula [15]:

$$E = \frac{1}{2}\omega^2(J_0 + \frac{3}{2}\omega^2 J_1)$$

Graph 7(b) shows that J_0 is very close to the MoI J displayed in Fig. 7(a). The J_1 parameter is related to the rigidity of the nucleus, relatively small J_1 values associ-

ated with large J_0 values indicating an increased rigidity (a behavior closer to that of rigid rotor). The variation of J_1 shown in graph 7(c) shows that the nuclei with P values above 3 show a rather monotonous decrease of J_1, indicating a rigidity that increases with the increase of the P-number. A detailed understanding of the behavior of J_1 is more difficult to achieve (see, for example, the discussion in [16]), but, as a partial conclusion, from graphs (a), (b), and (c) of Fig. 7 we can say that above $P \approx 6$, where J_0 stabilizes around half the rigid-body value, the nuclei of our set have the largest rigidity (or, they behave almost like a rigid rotor, in the sense that their intrinsic structure changes little with the excitation energy or rotation). The rest of three graphs in Fig. 7 show the evolution of different other structure indicators and strengthen this conclusion. The energy ratio $R(4/2) = E(4_1^+)/E(2_1^+)$ (graph (d)) evolves smoothly with P, and the transition towards good rotor ($R(4/2) > 3.27$) takes place around $P = 5$ as stated in [9]. The experimental quadrupole deformation β_2 (graph (e)) shows a smooth increase with P, reaching about 0.25 around $P = 5$. It is seen that β_2 has a very steep increase with $R(4/2)$ after $R(4/2) \gtrsim 3.27$ (graph (f)).

However, we could not correlate the behavior of the hindrance factors for the 4_1^+ and 6_1^+ states with any of these structure indicators. It remains to understand why this peculiar behavior takes place in the region where the nuclei are closest to rigid rotors.

5. CONCLUSIONS

We have studied the evolution of the known hindrance factors in the alpha-decay of the even-even trans-lead nuclei, for several excited states in the daughter nucleus, namely the 2_1^+, 4_1^+, 6_1^+, 0_2^+, and 1_1^+. The main results of this study are the following.

First, for the 2_1^+, 4_1^+ and 6_1^+ members of the ground state bands, the experimental values of the hindrance factors show rather compact systematics within the N_pN_n and P schemes of Casten [3, 9]. These systematics could be used for predicting fine structure alpha-decay branchings in nuclei where they are not measured. They may represent a useful alternative to the Geiger-Nuttall law approach that was recently shown to be valid for the hindered, fine structure transitions as well [17].

Second, the 2_1^+, 4_1^+, and 6_1^+ states show strikingly different behaviors. In particular, the behavior of the hindrance factors for the 4_1^+ and 6_1^+ states in the region of the nuclei showing the most rigid-rotor like behavior is very conspicuous and its understanding represents a big challenge for nuclear structure models.

Acknowledgments. We thank Dr. P-A. Söderström for the VMI model fits and useful discussion.

REFERENCES

1. H. Geiger and J.M. Nuttall, Philos. Mag. **22**, 613 (1911).
2. V.E. Viola and G.T. Seaborg, Nucl. Chem. **28**, 741 (1966).
3. R.F.Casten, Nucl. Phys. A **443**, 1 (1985).
4. Y.A. Ellis and M.R. Schmorak, Nuclear Data Sheets B **8**, 345 (1972).
5. Y.A. Akovali, Nuclear Data Sheets **84**, 1 (1998).
6. Evaluated Nuclear Structure Data File (ENSDF), maintained by the National Nuclear Data Center, Brookhaven National Laboratory: `http://www.nndc.bnl.gov/ensdf`.
7. M.A. Preston, Phys. Rev. **71**, 865 (1947).
8. R.F. Casten and N.V. Zamfir, Phys. Rev. Lett. **70**, 402 (1993).
9. R.F. Casten, D.S. Brenner, and P.E. Haustein, Phys. Rev. Lett. **58**, 658 (1987).
10. D.S. Delion, S. Peltonen, and J. Suhonen, Phys. Rev. C **73**, 014315 (2006).
11. S. Peltonen, D.S. Delion, and J. Suhonen, Phys. Rev. C **78**, 034608 (2008).
12. P. Möller, J.R. Nix, W.D. Myers, and W.J. Swiatecki, At. Data Nucl. Data Tables **59**, 185 (1995).
13. S. Raman, C.W. Nestor, Jr., and P. Tikkanen, Nuclear Data Tables **78**, 1 (2001).
14. S.G. Nilsson and I. Ragnarsson, *Shapes and shells in nuclear structure* (Cambridge Univ. Press, 1995).
15. M.A.J. Mariscotti, G. Scharff-Goldhaber, and B. Buck, Phys. Rev. **178**, 1864 (1969).
16. N. Rowley, J. Ollier, and J. Simpson, Phys. Rev. C **80**, 024323 (2009).
17. Xin Zhang, Chang Xu, and Zhongzhou Ren, Phys. Rev. C **84**, 044312 (2011).

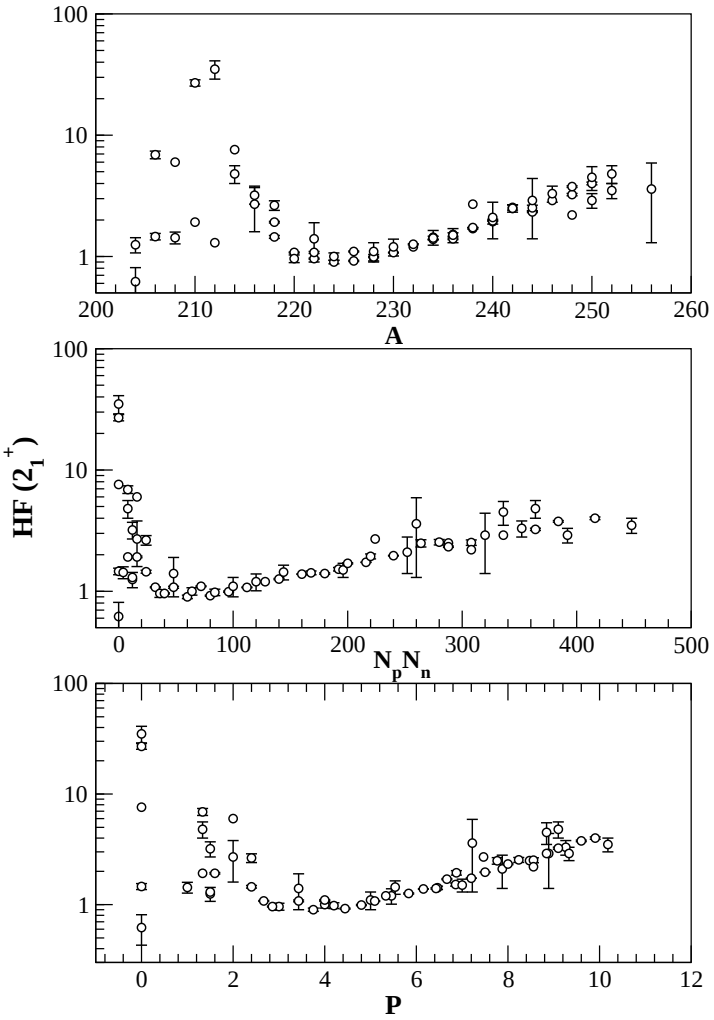

Fig. 1 – Hindrance factors for the 2_1^+ excited state as a function of mass number A (top panel), the quantity N_pN_n (middle), and $P = N_pN_n/(N_p + N_n)$ (bottom). See text for the definition of N_p and N_n. Here the mass number A and the N_p and N_n values are those of the daughter nuclei (see discussion in text).

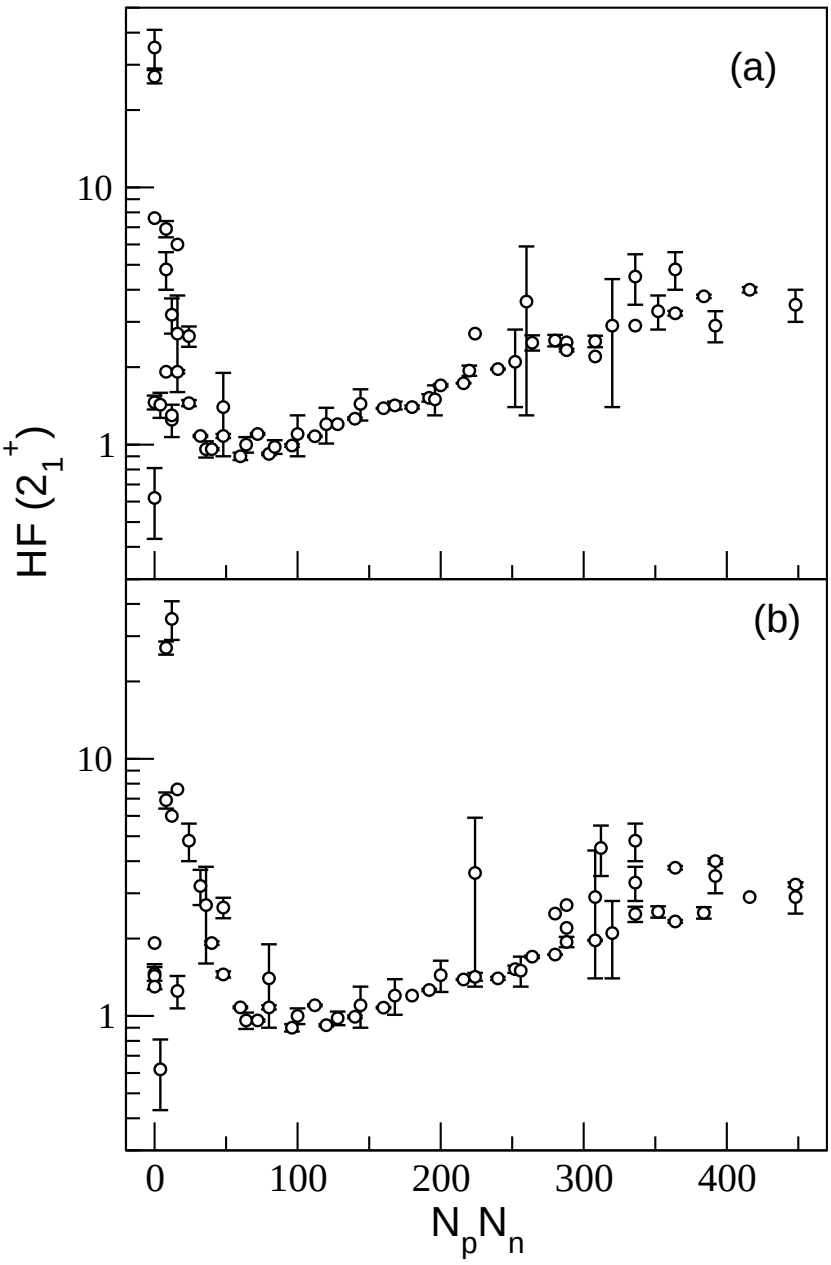

Fig. 2 – Hindrance factor for the 2_1^+ state, represented as a function of the product N_pN_n, with N_p, N_n calculated (a) for the daughter nuclei; (b): for the parent nuclei.

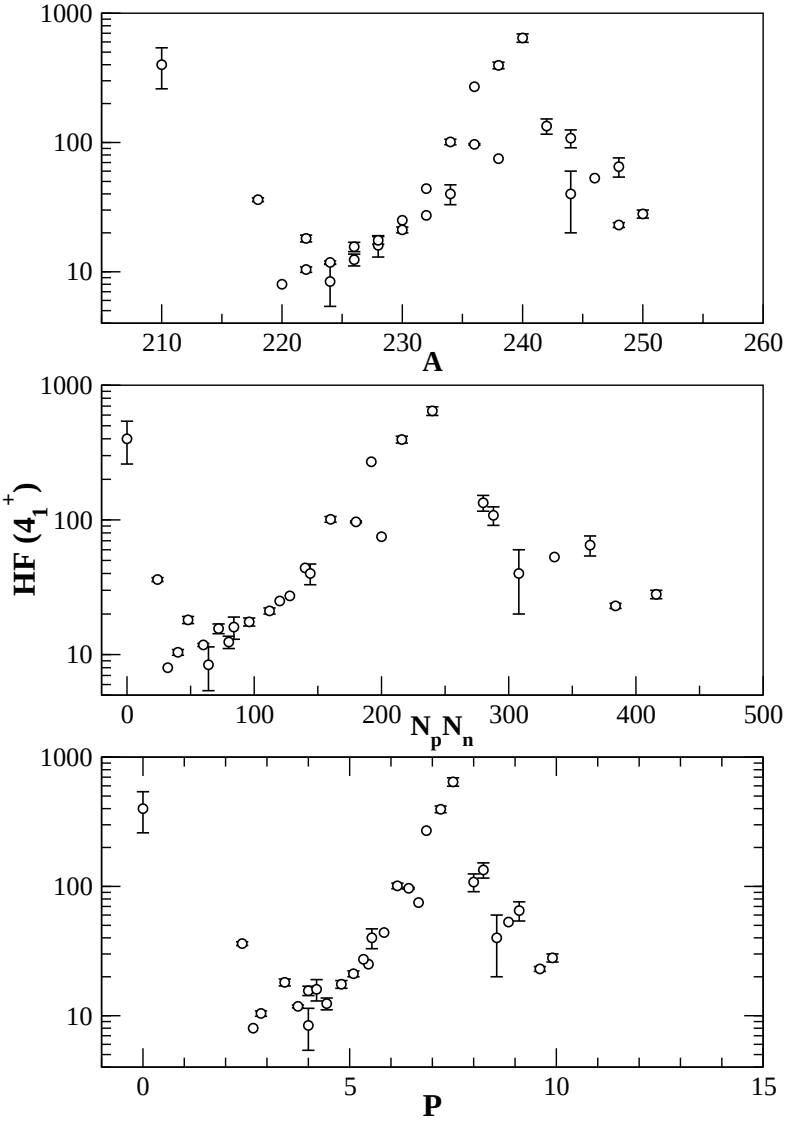

Fig. 3 – Same as Fig. 1, but for the 4_1^+ state.

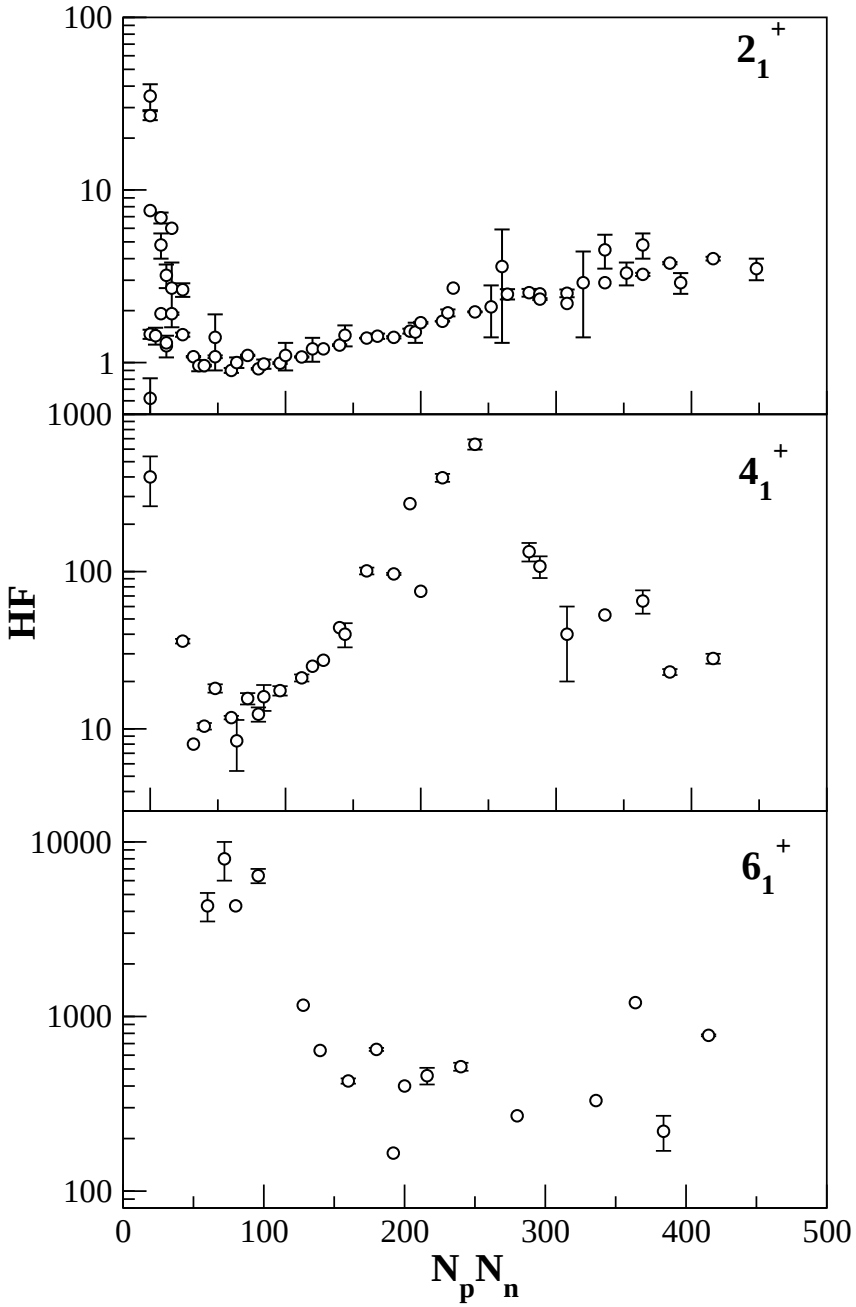

Fig. 4 – Comparison of the hindrance factors of the 2_1^+, 4_1^+, and 6_1^+ states as a function of the N_pN_n quantity.

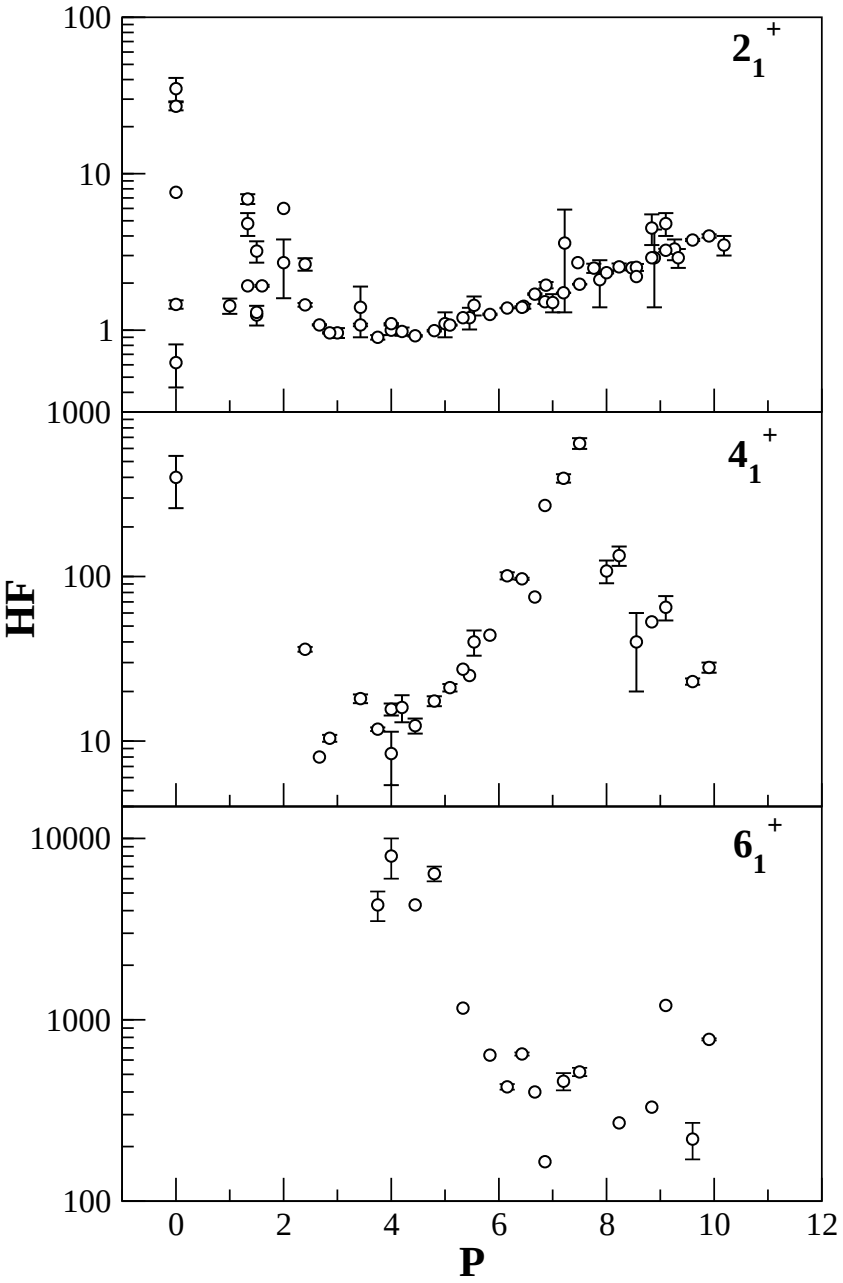

Fig. 5 – Same as Fig.3, but as function of the P quantity.

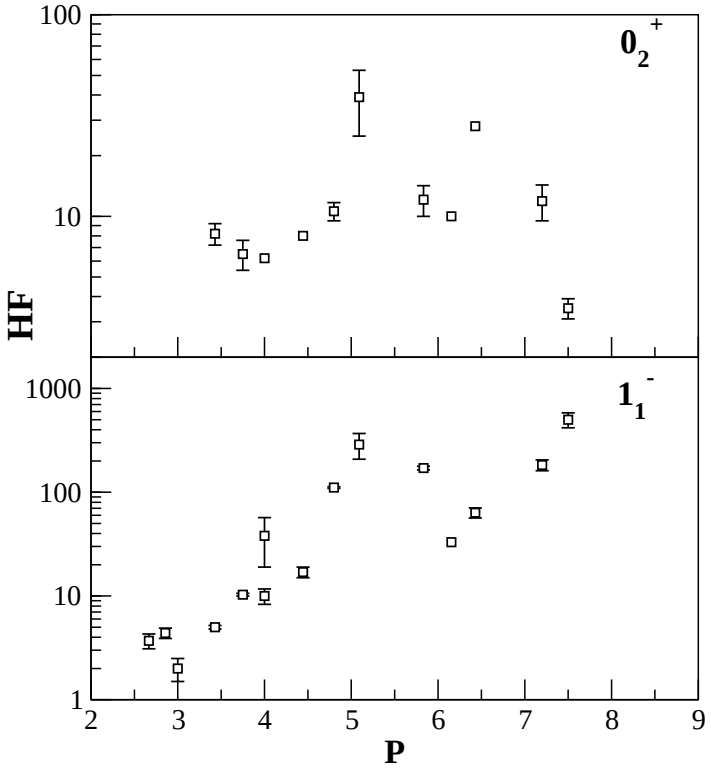

Fig. 6 – Hindrance factors of the 0_2^+ and 1_1^- excited states as a function of P.

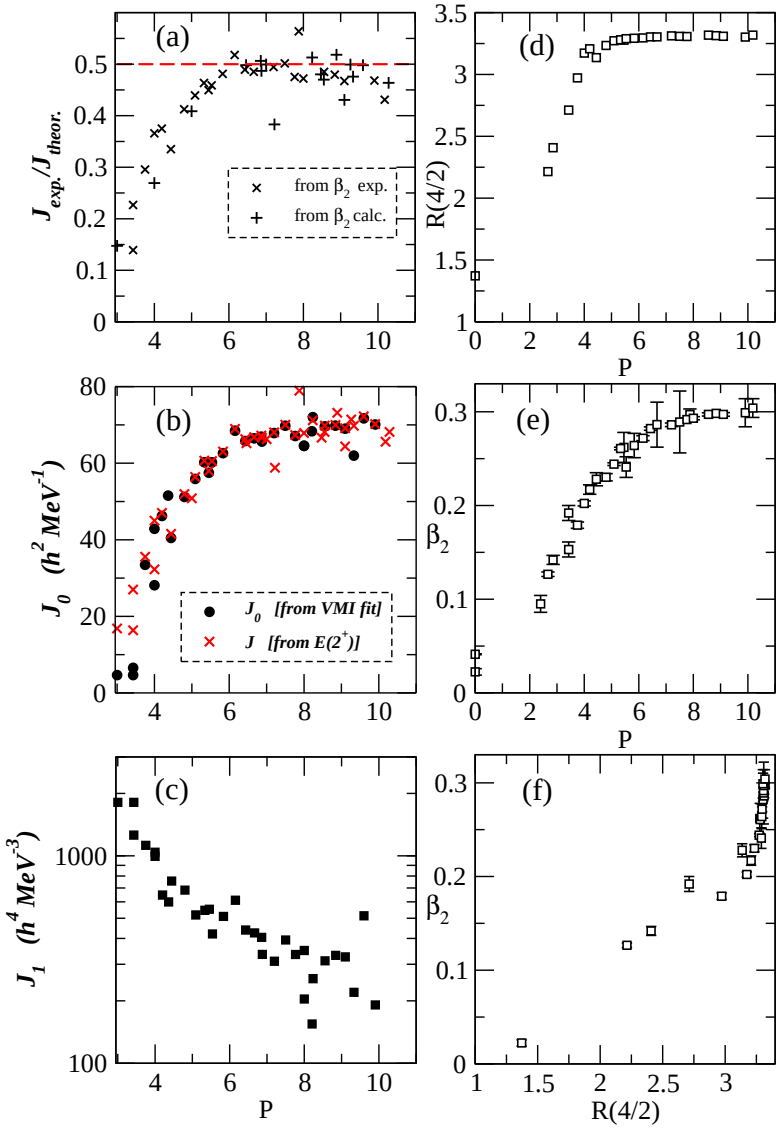

Fig. 7 – Evolution of different structure indicators of the considered nuclei (that is, those for which at least $HF(2_1^+)$ has been measured). (a) Ratio of the experimental moment of inertia (calculated form the energy of the 2_1^+ state) and the calculated one (corresponding to the β_2 quadrupole deformation (either experimental [13], or from [12]); (b) and (c): Harris parameters J_0 and J_1 from fits to the g.s.b. energies; J_0 is also compared to the moment of inertia extracted from the 2_1^+ energy; (d) $R(4/2) = E(4_1^+)/E(2_1^+)$ as a function of P; the experimental β_2 quadrupole deformation as a function of: (e) P, and (f) $R(4/2)$.